Mustansiriyah Journal of Materials Engineering and Sustainability
Volume 01, No. 01, 2025, Pages 36-47
https://mjmes.uomustansiriyah.edu.iq/
Research Article

DOI: https://doi.org/10.31272/abf5a358

ISSN: 3079-9899 (Print)
ISSN: 3079-9902 (Online)

Analyze Thermal Installation in Buildings for Different Insulations and Thicknesses Using Computational Fluid Dynamic

Afreen Emad Sa'ad-Aldeen [1*], Salwa Ahmad Sarow [2]

[1] Materials Engineering Department, College of Engineering, University of Mustansiriyah, Baghdad, Iraq
[2] Mechanical Engineering Department, College of Engineering, University of Mustansiriyah, Baghdad, Iraq
*Corresponding author: Email: engafreen@uomustansiriyah.edu.iq (https://orcid.org/0000-0001-7891-5823)

Article Info

Received	06/05/2025
Revised	27/06/2025
Accepted	28/06/2025
Published	01/07/2025

Abstract

The purpose of thermal insulation is to reduce the rate of heat transfer. The goal of this work is to investigate the impact of various insulator species that can be utilized to increase thermal insulation. In the present investigation, natural heat transfer investigations are accomplished with a wooden box enclosure and four insulating materials with different thermal conductivity and two thicknesses of 2 cm and 4 cm for each piece. Four pieces of insulating material are PE foam, Polyisocyanurate, Polystyrene (XPS 300) and wood that is each piece attached in the middle space of the wooden test cell to achieve two parts up and down flow region. The experimental work is done with heat flux (350,500 and 650W/m^2) and Ra numbers ranging from (2.19×105 to 1.30×10^6). Also, the wooden test cell is simulated using computational fluid dynamics by using 3D Fluent Ansys software program version 17.2 for temperature distribution through insulation and enclosure with heat flux (500 W/m2) and Ra numbers ranging from (2.19×105 to 1.30×106). The results are shown when there is a reduction in insulator conductivity, so a decrease in the heat transfer through the box walls results in preferable thermal insulation for the box. The relationship between thermal conductivity (k) and the optimum thickness of various insulation materials (t_{opt}) is investigated with a polynomial non-linear correlation. This correlation will be particularly useful in estimating the ideal thickness of insulators for minimizing heat transfer meanwhile an insulation material based solely on its thermal conductivity.

Keywords: Natural Convection, Thermal Conductivity, Turbulent, Numerical Analysis, Correlation of Optimum Thickness, Computational Fluid Dynamics.

1. Introduction

The global energy demand is growing and will continue to do so for the next twenty years. The world may not be able to meet its climate change targets or repair these concerns with adequate supplies due to the challenges of addressing suitable and shared energy policy [1]. Insulation material is commonly used to reduce heat transfer and enter a structure from the outside with an air conditioning apparatus. The heat conductivity of this substance is very low [2]. Conduction is used to move heat through insulating materials, while convection and radiation are used to transfer heat to or from the atmosphere. Insulation is a type of material that is used to reduce heat loss or gain in buildings and manufacturing operations [3]. Polyurethane (PU) foams are widely utilized as insulating and core materials in furniture, cooling and freezing systems, house construction, ship construction, piping, tank construction, etc. [4]. Appropriate insulation has an ideal insulation thickness and a total insulation expenditure cost that is lower than the entire investment cost for the insulation [5].

Several studies have looked into the idea of using thermal insulation in a variety of applications, according to past studies. Analyzed correlation by Mahlia, et al. 2007[5] between the thickness of selected insulation materials for building walls is proportional to their conductivity. The cost of insulation increased but the cost of cooling reduced with increased thermal resistance of insulation material, according to results. At the lower head of a pressure vessel, natural convection in a volumetrically heated fluid with properties similar to an oxide layer of a molten core was investigated by Vieira, et al. 2012[6]. Long and Ye 2015[7] studied the impact of wall materials' thermal conductivity and heat capacity volumetric on energy effectiveness. Through a traversing investigation and theoretical analysis with an active building, the functions of external and internal wall thermal insulation and heat storage

were clarified. A reduction in the room's cooling energy in the summer was caused by a decrease in conductivity or an increase in the volumetric heat capacity of the materials. Buyruk 2017[8] employed varying insulation thicknesses and examined them experimentally and numerically, taking into account different environmental temperatures. The Fluent program was used to calculate the contours of temperature and heat flux for external insulated cases with various thicknesses of insulation and interior temperatures. For all ambient temperatures and insulation thicknesses, in the vicinity of thermal bridges, substantial heat transfer rates were achieved.

Hasan, et al. 2018 [9] conducted an experimental study by adding layers of thermal insulation material to the walls and ceiling that used PCM as a thermal insulation material. Two models of rooms have been built: one was a conventional room, and the other testing room was used in experiments. The PCM utilized in this experiment was paraffin wax, which has a 44°C melting point. The use of PCM as insulation materials resulted in a reduction in the zone's indoor temperature, a decrease in cooling load, and, as a result, a decrease in energy consumption. Inside a compartment with thermally insulated walls, the temperature rises and falls was analyzed using a mathematical model by Hana, et al. 2018 [10]. The simulation results are then used to calculate the time required due to the low ambient temperature, and the required drop in air temperature inside the measured room during cooling.

Tsvetkov, et al. 2018 [11] simulated the usage of novel thermal-efficient construction materials in a layered of an external framed wall's non-uniform structure made of polystyrene concrete. The nature of a polystyrene concrete structure's temperature field distribution was established, and its thermal protection properties were explored. Numerical methods were used by Yuan 2018[12] to investigate the effects of thermal parameters, insulator species and thickness of exterior walls. Thermal transmittance, decrement factor or amplitude attenuation, time lag, thermal admittance, time lead for thermal admittance, surface factor, and thermal capacity were all investigated. Insulation type and thickness have been shown to affect thermal transmittance, decrement factor, and time lag, but not thermal admittance, time lead for thermal admittance, surface factor, or the thermal capacity of external wall constructions.

AIPs' thermal performance in terms of energy efficiency in buildings was examined numerically and empirically by Yang, et al. 2019 [13]. To assess and compare their thermal capabilities, three types of insulating cells were developed as insulator layers. When compared with typical insulating walls, the AIP wall reduced the variation range for the heat flowing and interior temperature by 40% and 20%, respectively.

An experimental investigation was conducted by Liu, et al. 2020[14] to evaluate the impacts of slab-edge insulation on enhancing the ground level's thermal performance and minimizing operating energy loss over the floor surface. In the study's testing module, it was discovered that more than 20% of heat loss via the ground level was minimized. Khairulmaini, et al. 2020[15] investigated the effect of various types of insulation materials that can be utilized to enhance the insulation material of cool boxes. As the thermal conductivity is minimal, results showed that heat transmission through the cool box's walls is likewise low, resulting in improved cool box thermal insulation. Many authors investigate transport phenomena problems using different simulations type such as computional fluid dynamics [18-20], comsol, Fluent Ansys software [21-22].

The current investigation aims to investigate the impact of various insulator materials that can be utilized to increase thermal insulation and reduce thermal loads. The natural heat transfer is being conducted with a wooden box enclosure and four insulating materials with different thermal conductivity and two thicknesses of 2 cm and 4 cm for each piece. Four pieces of insulating material are PE foam, Polyisocyanurate, Polystyrene (XPS 300) and wood that are attached in the middle space of the wooden test cell to achieve two parts up and down flow region. Also, the wooden test cell is simulated by using 3D Fluent Ansys software program version 17.2 to investigate temperature distribution through insulation and enclosure with heat flux (500 W/m2) and Ra numbers ranging from (2.19×105 to 1.30×106). The experimental work is done with heat flux (350,500 and 650W/m2) and Ra numbers ranging from (2.19×105 to 1.30×106). The results from experimental and numerical are analyzed.

2. Experimental work

2.1 Test section

Insulating cells made of a wooden box and insulating materials were developed for the aim of testing the insulating materials' thermal performance in an experimental setting. The dimension of the wooden box lined with aluminum foil to reject heat is (30×10×15) cm with a thickness of 5cm, as shown in Fig. 1. The Schematic diagram for the experimental test is shown in Fig.2. The upper surface of the wooden box is opening for ambient. Four pieces of insulating material with different thermal conductivity are PE foam, Polyisocyanurate, Polystyrene (XPS 300) and wood each piece is attached in the middle space of the wooden test cell to achieve two parts up and down flow region. The insulating materials are with dimensions of (10×15) cm, with two thicknesses (2cm and 4cm) for each piece. The thermal properties of insulating material are illustrated in Table 1. The bottom surface of up flow region contains a heater with power (100 W). For the thermal insulation test at ambient temperature (T∞= 27°C), the up flow region is started at 27°C until reaches a steady state and the down flow region is maintained at 27°C. The experimental work is done with heat flux (350,500 and 650W/m2) and Ra numbers ranging from (2.19×105 to 1.30×106). The experimental steady state condition within 30 minutes, the local temperatures of the model are recorded. **Fig.1** The form of the enclosure geometry

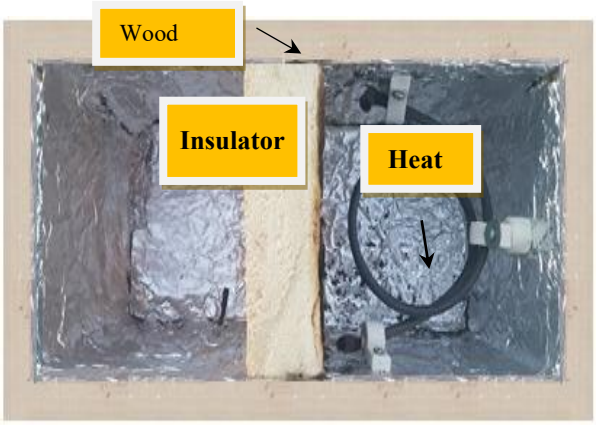

Fig 1. The form of the enclosure geometry

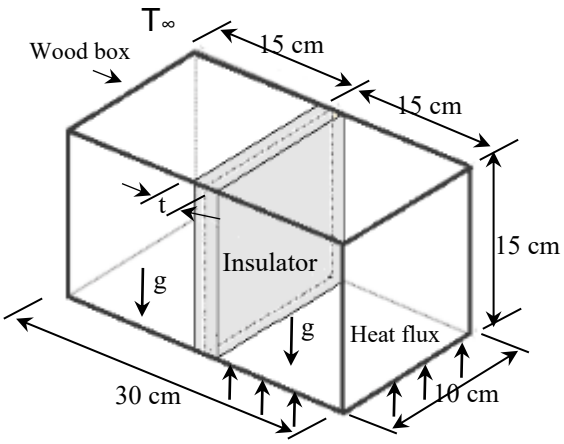

Fig 2. Schematic of enclosure geometry

Table 1. Properties of Spaceman.

	PE foam	Polyisocyanurate	Polystyrene (XPS 300)	wood
Thermal Conductivity (W/m.K)	0.02	0.032	0.08	0.15
Density (kg/m3)	12	30	32	750
Specific Heat (J/kg.K)	500	700	1900	1700

2.2 Measurement Devices and Test Procedure

Thermocouples (K-type) with temperature tolerance ranges of 0 to 350°C and 0.4 percent accuracies are used to assess the test section's internal air temperatures. Two K-type thermocouples (i.e., T1–T2) are fitted in the test section, one at the up flow region and another one at the down flow region. There are five thermocouples (T3–T7) positioned at the center of the insulator surface within thickness to detect the insulator surface temperature. The thermocouple setup can be seen in Fig. 3. The temperature recorder in this work is the data logger system (Lutron-Model BTM-4208SD) contains 12 channels and it has a digital screen to monitor the temperature of each thermocouple connected to each channel.

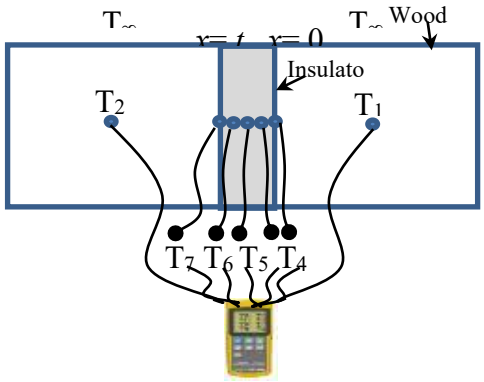

Fig 3. Schematic of thermocouple distribution

2.3 Data reduction:

A volumetric heated rectangular cavity with all isothermal walls (at T = 300K) with two regions, up flow region containing heat flux (350,500 and 650W/m2) and down flow region is maintained at 27°C. The physical problem used for the natural convection study with Ra numbers ranging from (2.19×105 to 1.30×106) and working fluid with Pr number equal to 0.7.

The dimensionless parameter that represents the natural convection effects is Grashof number (Gr) [16]:

$$Gr = \frac{g\beta(T_s - T_\infty)L_c^3}{\gamma^2} \quad (1)$$

The Rayleigh number (RaL) is the result of multiplying the Grashof and Prandtl numbers:

$$Ra_L = Gr\ Pr = \frac{g\beta(T_s - T_\infty)L_c^3}{\gamma^2} Pr \quad (2)$$

In order to predict the heat transfer rate, the Nusselt number is:

$$Nu = \frac{hl_c}{k} \quad (3)$$

$$Nu = C(Gr\ Pr)^n = CRa_L^n \quad (4)$$

The surface geometry and flow regime are based on the values of the constants C and n, which are defined by the Rayleigh number range. For laminar flow, n is normally 1/4 while for turbulent flow, it is 1/3. Normally, the value of constant C is less than one.

At the film temperature, all fluid properties are examined.

$$T_f = \frac{1}{2}(T_s + T_\infty) \quad (5)$$

Heat provided from the heater at up flow region base can be determined:

$$q_{heater} = I\,V$$

Newton's law of cooling expresses a uniform surface temperature (T_s) to the surrounding fluid as:

$$q_{conv} = q_{heater} = hA_s(T_\infty - T_{ins}) \quad (6)$$

The uncertainty is found in the maximum values of Nu number and Ra number thermal resistance are 3.86% and 2.88 %, respectively.

In order to calculate the heat transfer rate, the conduction and convection formula is employed through the insulation with thickness t. The following equation can be used to calculate the thermal transmission process via the insulator: [13]

$$q = UA(T_3 - T_7) \quad (7)$$

Where:

$$U = \frac{1}{R_T} \quad (8)$$

Total thermal resistance RT of the cell, calculated by [13]

$$R_T = \frac{1}{h_{in}} + \frac{t}{K_{ins}} + \frac{1}{h_o} \quad (9)$$

3. Numerical model

3.1 Physical model

In a rectangular wooden box, 3D-dimensional fluid flow and natural heat transfer characteristics are simulated using air as the working fluid. Fluent 17.2 is used to evaluate the problem mentioned with turbulent flow and constant heat flux. Heat flux in the up-flow region (500 W/m2) is simulated with two cases, case A which is heat flux at the left side and case B which is heat flux at the bottom region. The geometry of the wooden box with an air-filled enclosure is shown in Fig.4. A volumetric heated rectangular enclosure with all isothermal walls (at T = 300K), containing a working fluid with Pr number equal to 0.7 and Ra numbers ranging from 2.19×105 to 1.30×106. Four pieces of insulating material with different thermal conductivity are PE foam, Polyisocyanurate, Polystyrene (XPS 300) and wood that are attached in the middle space of the wooden test cell. All insulating materials are with dimensions of (10×15) cm, with two thicknesses (2cm and 4cm) for each piece.

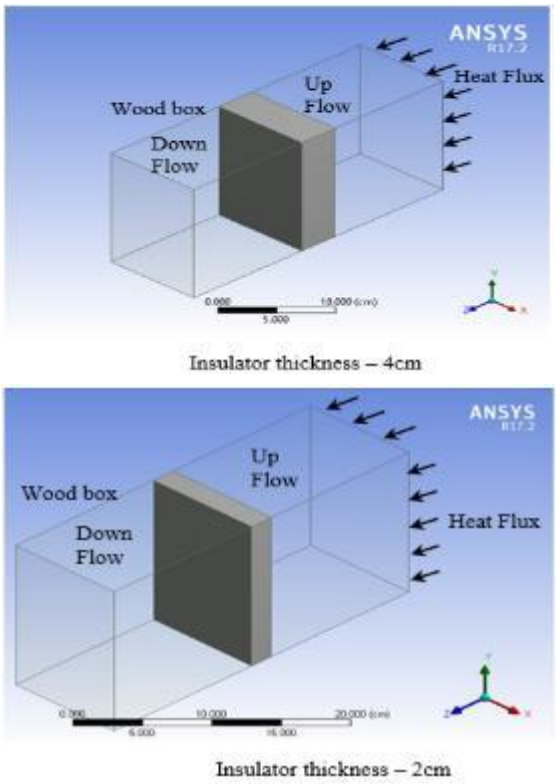

Case (A)

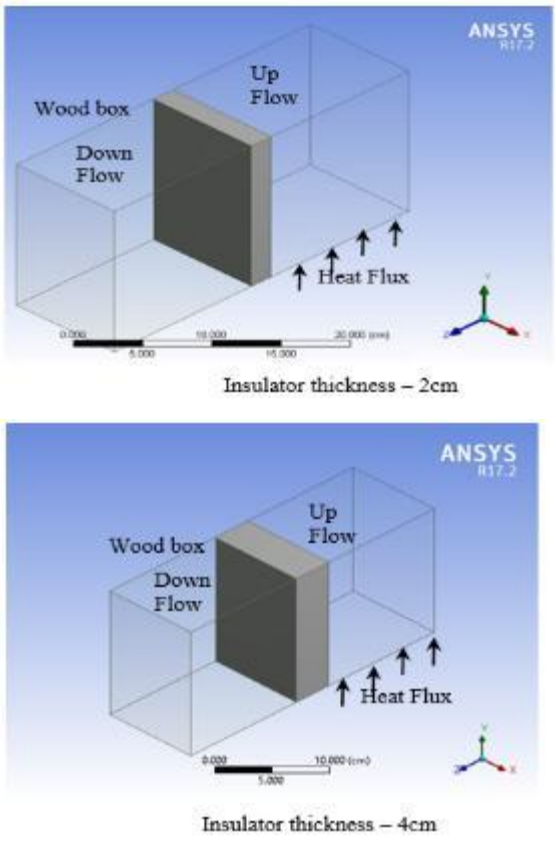

Case (B)

Fig 4. Schematic of the geometry of the wooden box

3.2 Mesh generation

Mesh sizes were performed for a rectangular wooden box to guarantee the grid independence of results. Fig.5 demonstrates the x,y, and z-direction computational grid for the geometrical model of the wooden box studied in this paper. A uniform grid with 157568 nodes is utilized in all of the calculations described in this paper, which was previously chosen via a mesh sensitivity study.

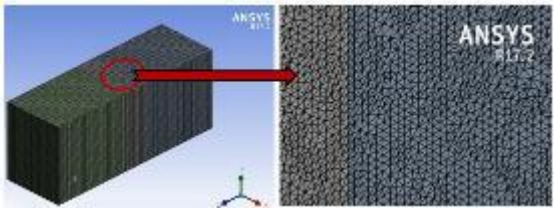

Fig.5 The mesh of the proposed geometry

3.3. Governing equations

A cartesian tensor method is used in this work with continuity, momentum, and energy equations to solve the numerical problem.
There are several simplifying assumptions: no-slip condition, steady state, incompressible fluid, turbulent flow through the box, uniform heat flux, continuous thermo-physical properties of solid and fluid and assuming the Bossiness approximation.

The three-dimensional Navier-Stokes governing equations using the standard k-ε model are:

For the fluid region, the mass continuity equation is [17]:

$$\frac{\partial u_x}{\partial x}+\frac{\partial u_y}{\partial y}+\frac{\partial u_z}{\partial z}=0 \quad (10)$$

For the fluid region the x- momentum equations [17]:

$$\frac{\partial u_x}{\partial x}+\frac{\partial u_y}{\partial y}+\frac{\partial u_z}{\partial z}=-\frac{1}{\rho_f}\frac{\partial p}{\partial x}+\nu\left(\frac{\partial^2 u_x}{\partial x^2}+\frac{\partial^2 u_y}{\partial y^2}+\frac{\partial^2 u_z}{\partial z^2}\right) \quad (11)$$

For the fluid region the y- momentum equations [17]:

$$\frac{\partial u_x}{\partial x}+\frac{\partial u_y}{\partial y}+\frac{\partial u_z}{\partial z}=-\frac{1}{\rho_f}\frac{\partial p}{\partial y}+\nu\left(\frac{\partial^2 u_y}{\partial x^2}+\frac{\partial^2 u_y}{\partial y^2}+\frac{\partial^2 u_y}{\partial z^2}\right)+\beta g(T-T_o) \quad (12)$$

For the fluid region the z- momentum equations [17]:

$$\frac{\partial u_x}{\partial x}+\frac{\partial u_y}{\partial y}+\frac{\partial u_z}{\partial z}=-\frac{1}{\rho_f}\frac{\partial p}{\partial z}+\nu\left(\frac{\partial^2 u_z}{\partial x^2}+\frac{\partial^2 u_z}{\partial y^2}+\frac{\partial^2 u_z}{\partial z^2}\right) \quad (13)$$

For the fluid domain, the energy equation is expressed as [17]:

$$\frac{\partial}{\partial x}(\rho u_x T)+\frac{\partial}{\partial y}(\rho u_y T)+\frac{\partial}{\partial z}(\rho u_z T)=\frac{\partial}{\partial x}\left[\rho(\alpha+\alpha_t)\frac{\partial T}{\partial x}\right]+\frac{\partial}{\partial y}\left[\rho(\alpha+\alpha_t)\frac{\partial T}{\partial y}\right]+\frac{\partial}{\partial z}\left[\rho(\alpha+\alpha_t)\frac{\partial T}{\partial z}\right] \quad (14)$$

Where: α_t is the turbulent thermal diffusivity:

$$\alpha_t=\frac{\nu_t}{Pr_t} \quad (15)$$

and Prt is the turbulent Prandtl number.

The last term in Eq. (12) is the Boussinesq buoyancy term, where [To= (Th + Tc)/2] is the reference temperature (i.e. the mean value of the hot wall temperature and the cold wall temperature), β is the volumetric expansion coefficient and g is the gravity acceleration.

The turbulence viscosity is assumed to be linked to the turbulence kinetic energy (k-equation) and the turbulence dissipation rate (ε -equation).

To get a fully converged solution, the residuals of the continuity, momentum, and energy equations must be less than 10-6.

3.4. Boundary conditions

The Boussinesq approximation is taken into consideration, and the model is deployed with full buoyancy and thermal effects. The boundary values for the velocity components and the turbulent kinetic energy are set to zero.
Boundary conditions have been applied to the top, bottom left and right walls of the domain. The top P=Pout, ux = uy = uz = 0.

At the bottom wall, boundary conditions at the heat flux surface are:

$$ux=uy=uz=0,\frac{\partial T}{\partial z}=0$$

while the walls are kept at uniform temperatures. The temperature of the up-flow region starts at 310K (Th) and down down-flow region is maintained at 300 K (Tc). The conduction inside the walls is through the insulator. Radiation effects were neglected.

4. Results and discussion

4.1. Experimental results

Experimental results for external and inner surface temperatures of the insulation cell, based on thermocouple T1-T7 observations are displayed in Fig. 6. The tests were carried out on four samples of insulator-type cells. Also for each sample, two alternative thicknesses were tested. The insulating materials with different thermal conductivity are PE foam, Polyisocyanurate, Polystyrene (XPS 300) and wood with two thicknesses (2cm and 4cm) for each sample.
The cells' outside surface temperatures were all 27°C at first, but they quickly increased. The experimental work is done with heat flux (350,500 and 650W/m2) and Ra numbers ranging from (2.19×105 to 1.30×106). Fig.6 demonstrates the experimental data of insulator surface temperatures through two thicknesses (2cm and 4cm) is seen that the temperature decreased when insulation thickness increased from (x = 0 to x = t) due to the heat resistance increased inside the insulation material

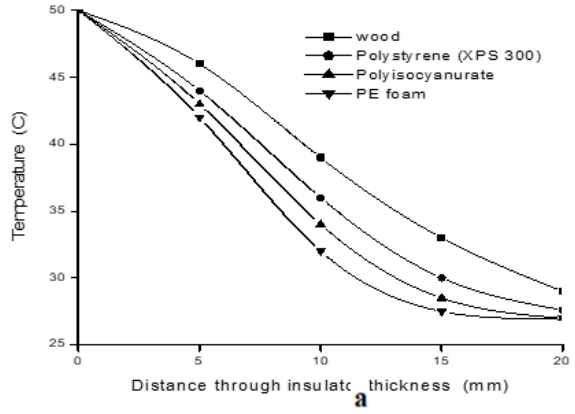

Fig 6. Temperature distribution through insulation thicknesses with heat flux (500W/m2): a-2cm, b- 4cm.

The total resistance and overall heat transfer coefficient of insulated materials are shown in Fig. 7 and Fig. 8 for insulation materials with (2cm and 4cm), respectively. The overall resistance is equal to the sum of the surface convective heat transfer resistances on the outer insulated surfaces and the interior resistances of the insulator layer. It can be seen in Fig. 7 and Fig. 8, the lower the thermal resistance insulation material, the lower the overall heat transfer coefficient as foam, and the highest the overall heat transfer coefficient as wood.

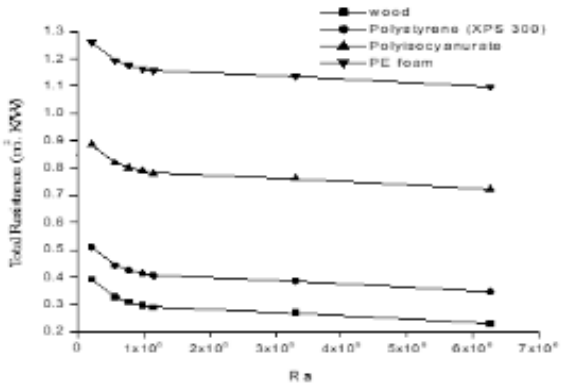

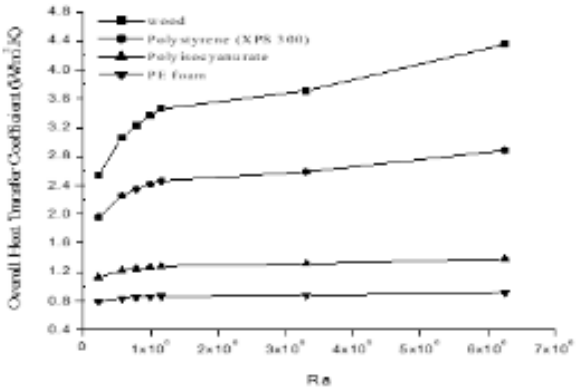

Fig 7. The total resistance and overall heat transfer coefficient of insulated materials with 2cm thickness

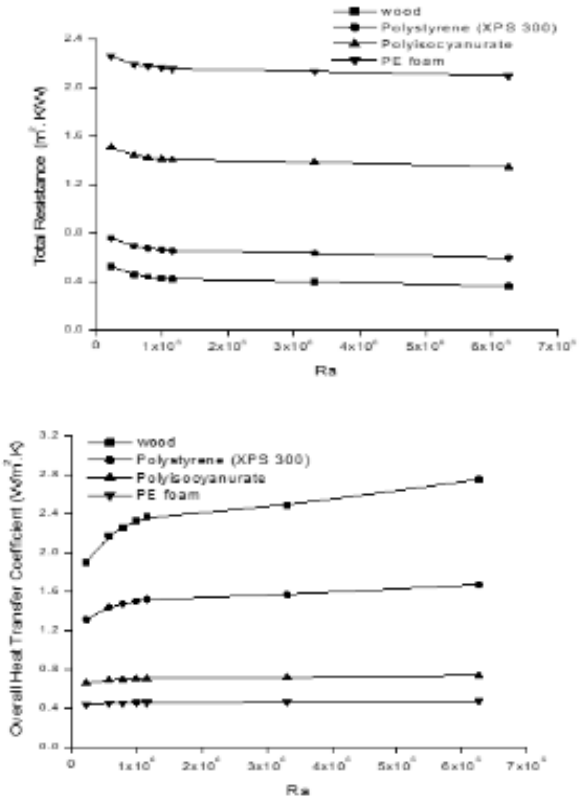

Fig 8. The total resistance and overall heat transfer coefficient of insulated materials with 4cm thickness

It is obvious in Fig. 9 that the Nusselt number and heat transfer coefficient in up flow region showed a great dependency on the Rayleigh number and heat flux.

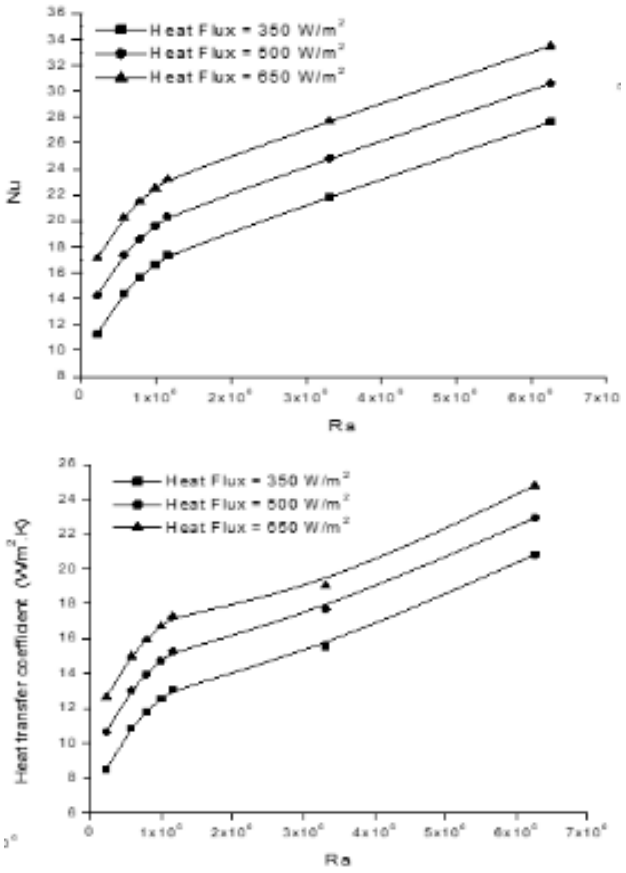

Fig 9. The Nusselt number and heat transfer coefficient in up flow region

4.2. Optimum insulation thickness correlation

Optimal thickness is necessary in the appropriate insulation material in order to possess an economical system. The thickness of the insulation will lower the cost of energy. This can be accomplished by determining the ideal thickness of the insulation material.

The relationship between thermal conductivity and insulation material thickness is investigated. The relationship between thermal conductivity (k) and the optimum thickness of various insulation materials (topt) is investigated with a polynomial non-linear correlation:

$$t_{opt.} = A + BK + CK^2$$

The optimal insulation thickness correlation can be determined in meters by using LAB Fit software as seen in Fig. 10 with the correlation as below:

$$t_{opt.} = 0.0074 + 0.915K - 2.893K^2$$

This correlation with $R^2 = 0.903$ will be very beneficial in estimating the ideal insulator thickness that can minimize the rate of heat transfer through the insulator based solely on its thermal conductivity.

Fig.11 shows the effect of the thermal conductivity of insulation used in this study to estimate the optimum thickness of insulation material from the correlation above.

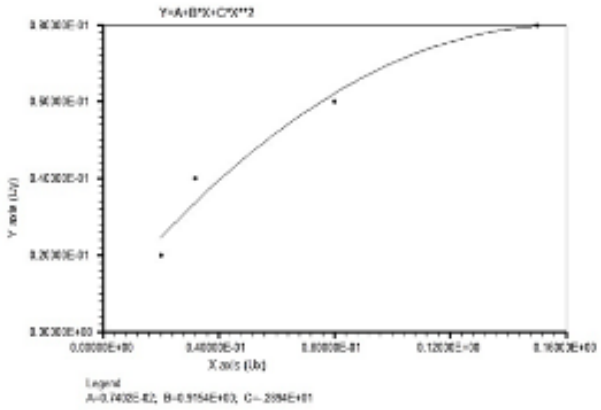

Fig 10. LAB Fit software results

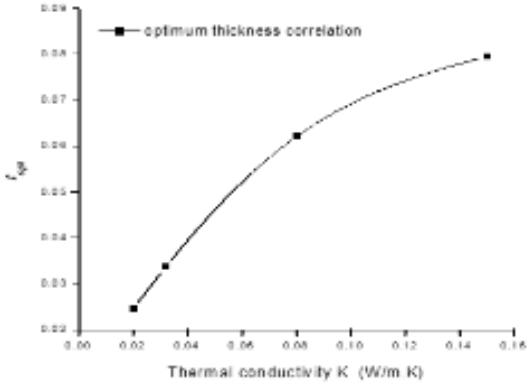

Fig 11. The thermal conductivity and optimum thickness (topt.) of insulation material

4.3. Numerical results

Numerical simulations are studied four pieces of insulating material PE foam, Polyisocyanurate, Polystyrene (XPS 300) and wood by using numerical ANSYS FLUENT version 17.2 software with standard k-ε for turbulence model. The four insulating materials have dimensions of (10×15) cm, with two thicknesses (2cm and 4cm). The local distributions of temperatures with various insulation types are studied. The insulating materials and wooden box temperature contours at heat flux (500W/m2) and Ra numbers ranging from (2.19×105 to 1.30×106) are done.

Fig.12 shows temperature variations for different foam insulation thicknesses (2cm and 4cm) in case there is heat flux on the left side. As seen from Fig.12, the temperature values decrease linearly from the inside insulator surface (up flow region) to the insulator where maximum heat resistance inside the insulation material and in the outer insulator, the values of surface temperature decrease to 27°C temperature value. Heat losses decrease as insulation thickness rises, as shown in Fig.12.

So, a more effective insulator with increased thickness is formed.

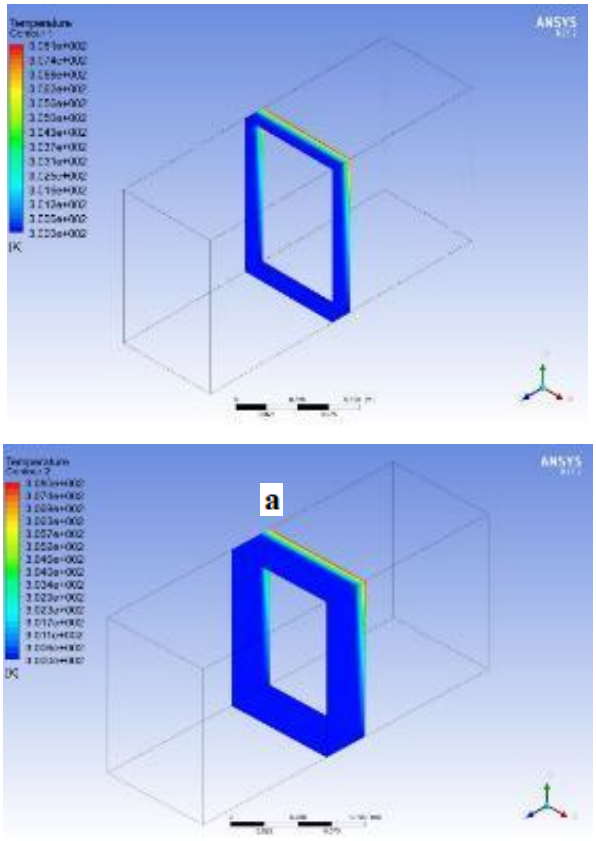

Fig 12. Temperature distribution through foam insulation thicknesses: a-2cm, b- 4cm.

Fig.13 shows the temperature distribution for the case that is heat flux on the left side, in the up and down flow regions of 2cm and 4cm foam respectively, the temperature in the up-flow region started at 27 C and then increased gradually until reaching steady state.

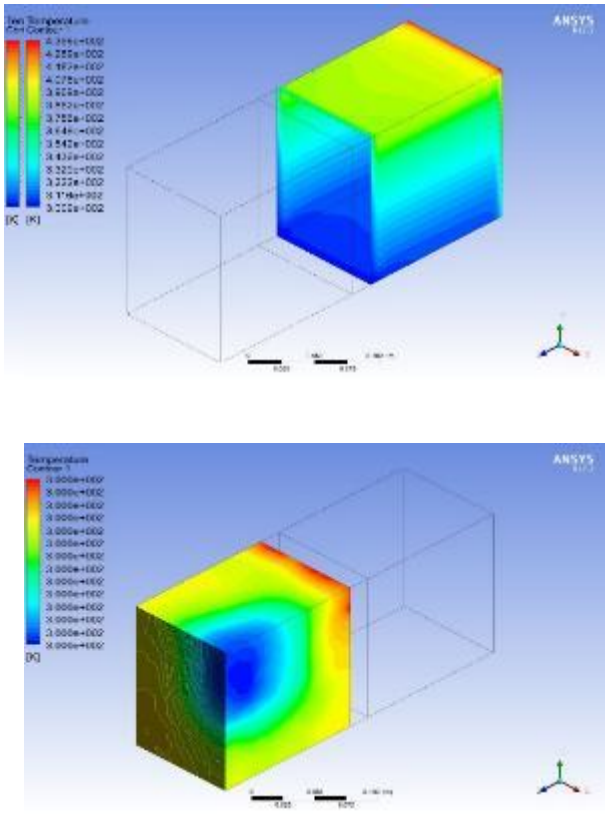

Fig 13. Temperature distribution in up and down flow region with foam insulation thicknesses: a-2cm, b- 4cm

Fig.14 shows temperature variations for different polyisocyanurate insulation thicknesses (2cm and 4cm) in case there is heat flux on the left side. As can be seen from Fig.14, the values of surface temperature decrease from the surface of the internal insulator (upper flow region to the down flow region) and we show that the temperature gradient increases through the insulator to reach the insulator to reach 27.7°C and 27°C on the insulator surface in down flow region respectively due to the decrease in the heat resistance inside the insulation material. The heat flow vectors for 2 cm insulation are more intense than for 4 cm insulation due to insulation with a thickness of 4 cm has higher thermal resistance. In outer polyisocyanurate insulation, the temperature values reduce to 28°C temperature value on the insulator surface in the downflow region.

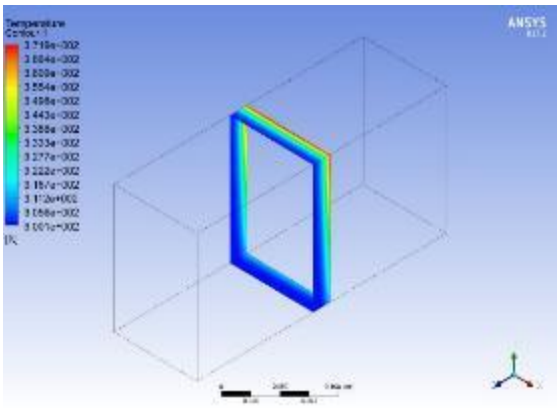

Fig 14. Temperature distribution through polyisocyanurate insulation thicknesses: a-2cm, b- 4cm.

Fig.15 shows temperature variations for different Polystyrene (XPS 300) insulation thicknesses (2cm and 4cm) in case there is heat flux on left side. It can be seen that the temperature gradient increases through the insulator to reach 30°C and 28°C on the insulator surface in down flow region respectively due to the decrease in the heat resistance inside the insulation material. The heat resistance is decreased through Polystyrene (XPS 300) insulation due to the increase in thermal conductivity (0.08 W/m.K).

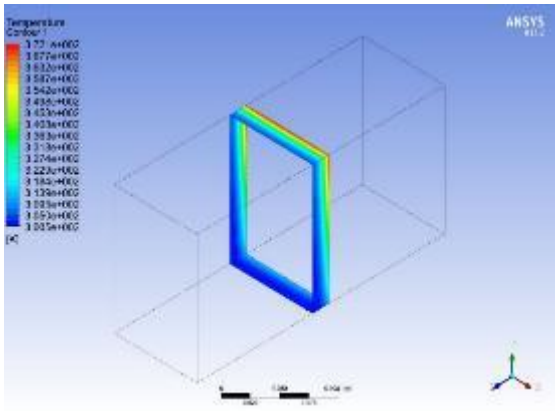

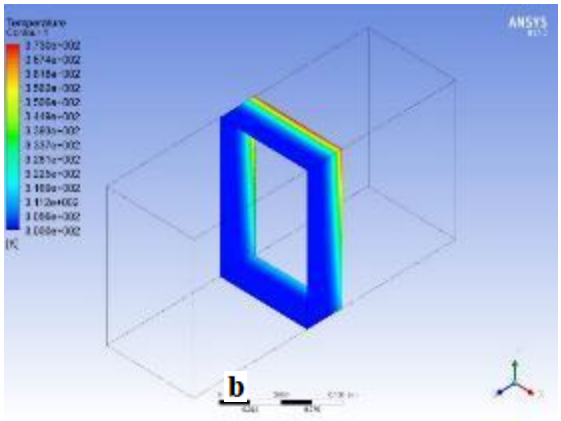

Fig 15. Temperature distribution through Polystyrene (XPS 300) insulation thicknesses: a-2cm, b- 4cm.

Fig.16 shows temperature variations for different wood insulation thicknesses (2cm and 4cm) in case there is heat flux on the left side. It can be seen that the temperature gradient increases through the insulator to reach 55°C and 30°C on the insulator surface in the down flow region in 2cm and 4cm respectively due to the decrease in the heat resistance inside the insulation material. The heat resistance is decreased through wood insulation due to the increase in thermal conductivity (0.15 W/m.K).

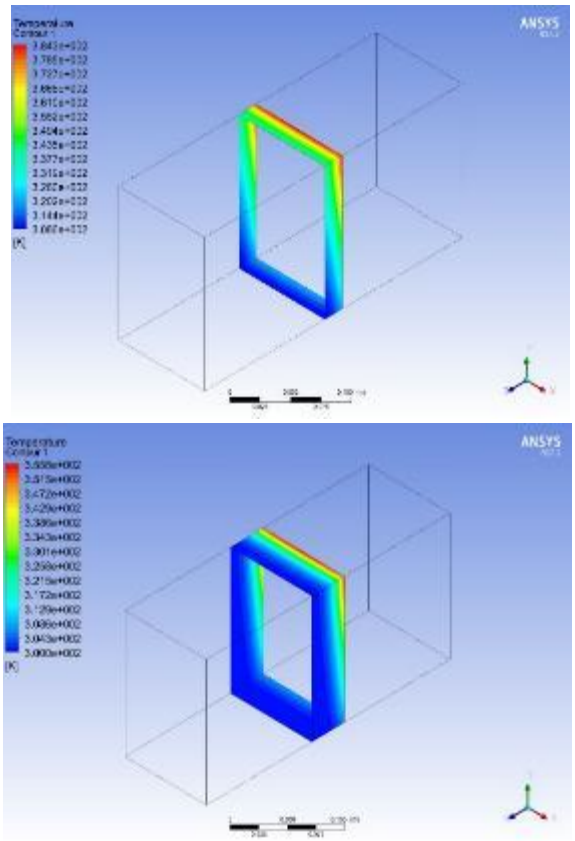

Fig 16. Temperature distribution through wood insulation thicknesses: a-2cm, b- 4cm.

Fig.17 shows the temperature distribution for the case that is heat flux at the left side and down the bottom in the up-flow region with heat flux (500 W/m2) with 4cm wood insulation, the temperature in the up-flow region is started at 27oC, and then increased gradually until reaching steady state.

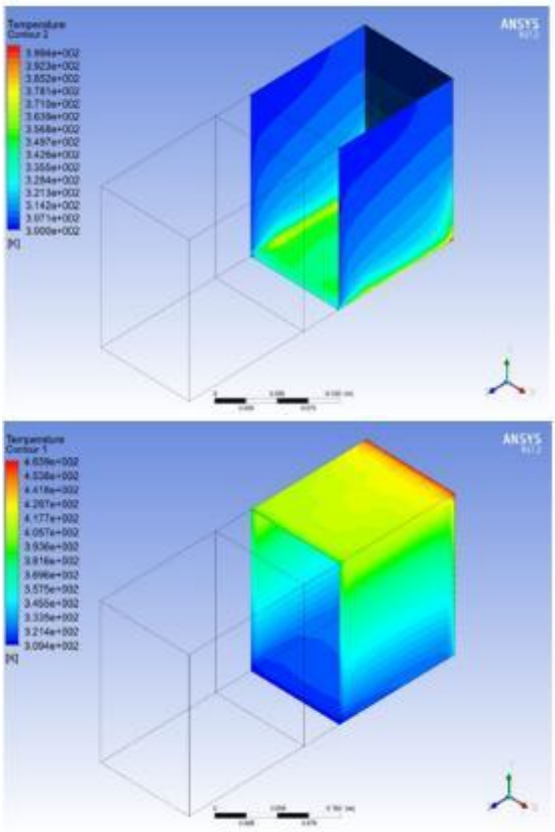

Fig 17. Temperature distribution through wood insulation thicknesses 4cm: a left side heat flux, b- down bottom heat flux

4.3. Turbulence eddy dissipation

Fig.18 shows the turbulence eddy dissipation that is the conversion of kinetic energy into heat is described by a turbulent flow characteristic because of the creation of eddies of different scales. In down flow region, there is no external energy added to the flow, but the flow's intensity will decrease over time, and it will lose its turbulent properties.

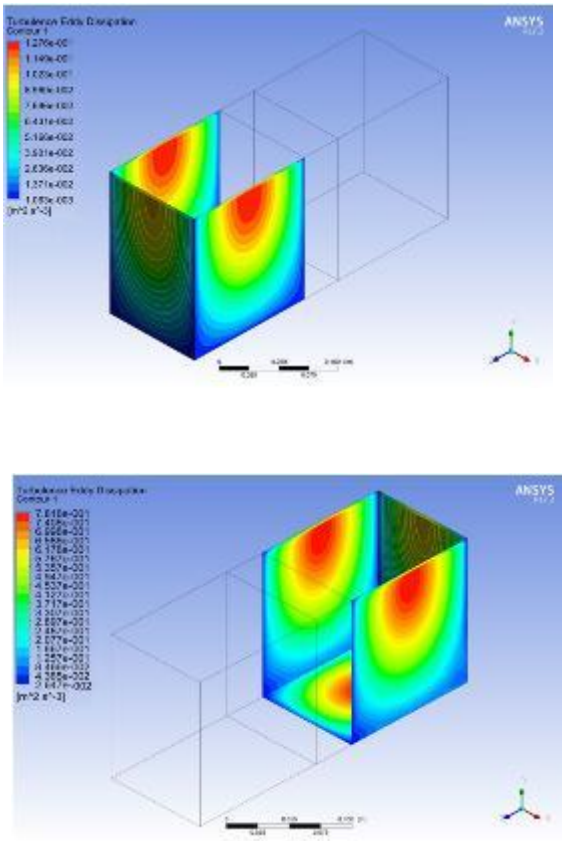

Fig 18. Turbulence eddy dissipation in up and down flow regions

5. CONCLUSIONS

The importance of energy in the development of technology is growing by the day. Thermal insulation is the most important aspect of energy conservation in buildings. In this work, the impact of varied thermal insulation material thicknesses and thermal conductivity on energy savings is investigated.
Different thicknesses (2 and 4 cm) of PE foam, Polyisocyanurate, Polystyrene (XPS 300), and wood are applied. Temperature distribution through insulation materials with different thicknesses are simulations by using Fluent program 17.2.
Our experimental results show that the overall heat transfer coefficient decreases with thickness increase, as the insulating material's thermal resistance improves. The obtained numerical results show temperature variations for different insulation and thicknesses; the temperature values decrease linearly from the surface of the internal insulator (in the upper flow region) to the external insulator surface (down flow region). A study of the correlation between thermal conductivity and the thickness of various insulator materials was conducted.

Nomenclatur

A_s Surface area, (m^2)
C Specific heat, (kJ/kg.k)
g Gravitational acceleration vector, (m/s^2)
Gr Grashof number
h Convection heat transfer coefficient, ($W/m^2.K$)
K Thermal conductivity, (W/m.K)
K_{ins} Thermal conductivity of the insulating, (W/m.K)
Nu Nusselt number
Pr Prandtl number
q Heat load, (W)
R Resistance of insulator, ($m^2.K/W$)
Ra Rayleigh number
t Insulator thickness, (m)
T Temperature, (^oC)
t_{opt} Optimum insulator thickness, (m)
U Overall heat transfer coefficient, ($W/m^2.K$)
x Coordinate along wall thickness, (m)
Δ Difference
μ Viscosity, (pa.s)
ρ Air density, (kg/m^3)
α The volume fraction

References

[1] F. Bisegna *et al.*, "Influence of Insulating Materials on Green Building Rating System Results," *Energies,* vol. 9, no. 9, p. 712, 2016, doi: https://doi.org/10.3390/en909071.

[2] M.-J. Park, J.-H. Song, J.-H. Lim, and S.-Y. Song, "Analysis of Needs for Building Envelope Insulation Regulations Reflecting the Thermal Bridging Effects through Similar Regulations Review and Case Study," (in Ko), *Journal of the Architectural Institute of Korea Planning & Design,* vol. 31, no. 2, pp. 303-312, 02/28 2015, doi: https://doi.org/10.5659/JAIK_PD.2015.31.2.303.

[3] D. K. Sahu, P. K. Sen, G. Sahu, R. Sharma, and S. Bohidar, "A review on thermal insulation and its optimum thickness to reduce heat loss," *Int. J. Innov. Res. Sci. Technol,* vol. 2, no. 6, pp. 2349-6010, 2015.

[4] S. H. Kim, H. C. Park, H. M. Jeong, and B. K. Kim, "Glass fiber reinforced rigid polyurethane foams," *Journal of Materials Science,* vol. 45, no. 10, pp. 2675-2680, 2010/05/01 2010, doi: https://doi.org/10.1007/s10853-010-4248-3.

[5] T. M. I. Mahlia, B. N. Taufiq, Ismail, and H. H. Masjuki, "Correlation between thermal conductivity and the thickness of selected insulation materials for building wall," *Energy and Buildings,* vol. 39, no. 2, pp. 182-187, 2007/02/01/ 2007, doi: https://doi.org/10.1016/j.enbuild.2006.06.002.

[6] C. B. Vieira, B. Niceno, and J. Su, "Computational Simulation of Turbulent Natural Convection in a Volumetrically Heated Square Cavity," in *2013 21st International Conference on Nuclear Engineering*, Chengdu, China, July 29–August 2, 2013 2013, vol. Volume 3: Nuclear Safety and Security; Codes, Standards, Licensing and Regulatory Issues; Computational Fluid Dynamics and Coupled Codes, V003T10A020, p. V003T10A020, doi: https://doi.org/10.1115/ICONE21-15486. [Online]. Available: https://doi.org/10.1115/ICONE21-15486

[7] L. Long and H. Ye, "Effects of Thermophysical Properties of Wall Materials on Energy Performance in an Active Building," *Energy Procedia,* vol. 75, no. 8, pp. 1850-1855, 2015/08/01/ 2015, doi: https://doi.org/10.1016/j.egypro.2015.07.161.

[8] E. Buyruk, F. Kılınc, K. Karabulut, M. Caner, and A. Bostancı, "Investigation of the Effect of Insulation Thickness on Energy Saving by Using Thermography," in *8th International Advanced Technologies Symposium, Elazığ, Turkey*, Elazig, Turkey, 19-22 October 2017, pp. 1611-1619.

[9] M. I. Hasan, H. O. Basher, and A. O. Shdhan, "Experimental investigation of phase change materials for insulation of residential buildings," *Sustainable Cities and Society,* vol. 36, no. 1, pp. 42-58, 2018/01/01/ 2018, doi: https://doi.org/10.1016/j.scs.2017.10.009.

[10] H. Charvátová, A. Procházka, and M. Zálešák, "Computer Simulation of Temperature Distribution during Cooling of the Thermally Insulated Room," *Energies,* vol. 11, no. 11, p. 3205, 2018, doi: https://doi.org/10.3390/en11113205.

[11] N. Tsvetkov, A. Khutornoi, A. Kozlobrodov, S. Romanenko, Y. Shefer, and A. Golovko, "Influence of metal frame on heat protection properties of a polystyrene concrete wall," *MATEC Web Conf.,* vol. 143, no. 1, p. 01005, 2018, doi: https://doi.org/10.1051/matecconf/201814301005.

[12] J. Yuan, "Impact of Insulation Type and Thickness on the Dynamic Thermal Characteristics of an External Wall Structure," *Sustainability,* vol. 10, no. 8, p. 2835, 2018, doi: https://doi.org/10.3390/su10082835.

[13] J. Yang *et al.*, "Numerical and experimental study on the thermal performance of aerogel insulating panels for building energy efficiency," *Renewable Energy,* vol. 138, no. 8, pp. 445-457, 2019/08/01/ 2019, doi: https://doi.org/10.1016/j.renene.2019.01.120.

[14] Z. Liu, D. Alterman, A. Page, B. Moghtaderi, and D. Chen, "An experimental study on the thermal effects of slab-edge-insulation for slab-on-grade housing in a moderate Australian climate," *Energy and Buildings,* vol. 235, no. 3, p. 110675, 2021/03/15/ 2021, doi: https://doi.org/10.1016/j.enbuild.2020.110675.

[15] M. Khairulmaini, Z. Michael, M. A. M. Shah, M. S. Zakaria, B. Abdullah, and A. A. Rashid, "Improvement of Insulation Material for Cool Box Application," *IOP Conference Series: Materials Science and Engineering,* vol. 834, no. 1, p. 012019, 2020/04/01 2020, doi: https://dx.doi.org/10.1088/1757-899X/834/1/012019.

[16] J. P. Holman, *Heat Transfer*, 10th ed. New York: McGraw-Hill Inc., 2010, p. 752.

[17] A. T. Skyllakos, A. E. Filios, D. P. Margaris, and M. G. Vrachopoulos, "CFD evaluation for turbulent

natural convection in rectangular enclosures," in *3rd International Conference on Experiments / Process / System Modeling / Simulation & Optimization*, Athens, 8-11 July, pp. 1-8.

[18] S. S. Muhsun, S. A. Talab Al-Osmy, S. A. M. Al-Hashimi, and Z. T. Al-Sharify, "Theoretical, CFD Simulation and Experimental Study to Predict the Flowrate Across a Square Edge Broad Crested Weir Depending on the End Depth as a Control Section," in *AWAM International Conference on Civil Engineering (AICCE'19)*, Penang, Malaysia, 2020: Springer International Publishing, in Proceedings of AICCE'19, pp. 15-34.

[19] S. M. Saleh, S. H. Muhammad, and A. A. Abo, "Effect of pooled and flat stepped spillway on energy dissipation using computational fluid dynamics," *Tikrit Journal of Engineering Sciences,* vol. 29, no. 2, pp. 75-79, 2022, doi: http://doi.org/10.25130/tjes.29.2.9.

[20] N. Q. Hussein, S. S. Muhsun, Z. T. Al-Sharify, and H. T. Hamad, "Unsteady state contaminants transport in sandy mediums using CFD model," *IOP Conference Series: Earth and Environmental Science,* vol. 779, no. 1, p. 012069, 2021/06/01 2021, doi: https://doi.org/10.1088/1755-1315/779/1/012069.

[21] S. S. Muhsun, Z. T. Al-Sharify, and H. M. Bahiya, "Simulation of two-phase flow contaminates transport in pipe flow under transient laminar flow condition," *Journal of Green Engineering,* vol. 10, no. 6, pp. 3861-3883, 2020.

[22] S. S. Muhsun and Z. T. Al-Sharify, "CFD simulated model and experimental tests for critical depth and flowrate estimation over a broad-crested weir under the longitudinal slope effect," *International Journal of Environment and Waste Management,* vol. 28, no. 1, pp. 41-60, 2021, doi: https://doi.org/10.1504/ijewm.2021.117006.